

**Pitfalls in the Synthesis of Polyimide-linked Two-dimensional Covalent Organic Frameworks**

Journal:	<i>Journal of Materials Chemistry A</i>
Manuscript ID	TA-ART-03-2021-001954.R2
Article Type:	Paper
Date Submitted by the Author:	08-Jun-2021
Complete List of Authors:	Kuehl, Valerie; University of Wyoming College of Arts and Sciences Wenzel, Michael; University of Wyoming College of Arts and Sciences Parkinson, Bruce; University of Wyoming College of Arts and Sciences, Department of Chemistry Sousa Oliveira, Laura; University of Wyoming College of Arts and Sciences, Department of Chemistry Hoberg, John; University of Wyoming College of Arts and Sciences,

ARTICLE

Pitfalls in the Synthesis of Polyimide-linked Two-dimensional Covalent Organic Frameworks

Received 00th January 20xx,
Accepted 00th January 20xx

Valerie A. Kuehl,^a Michael J. Wenzel,^a Bruce A. Parkinson^{a,b} Laura de Sousa Oliveira,^a and John O. Hoberg^{a*}

DOI: 10.1039/x0xx00000x

Abstract: The well-known reaction of amines with carboxylic acid anhydrides to produce highly stable imide moieties has been extended in the literature to the synthesis of two dimensional polyimide-linked covalent organic frameworks (2D-COFs). We report a detailed study of these reactions to determine whether the reported polymerizations are producing the reported COFs. The studies include variations of reaction temperature, time, heating method, and monomer structures to establish whether formation of ordered crystalline material is occurring. The results of these studies indicate that a specific, previously reported polyimide COD is likely not produced with the order or exact structure as reported.

Introduction Two-dimensional covalent organic frameworks (2D-COFs) are highly-ordered polymers with a well-defined pore structure and are of interest for numerous applications that include gas storage and separations,^{1,2} liquid and solute separations,^{3,4} catalysis,^{5,6} and optoelectronics.^{5,7} Investigations of COFs have undergone rapid growth over the past decade since reports of the self-condensation of boronic acids to form boronate ester COFs.⁸ Among these developments have been polyimide-linked COFs (PI-COFs) that are synthesized through the reaction of primary amines with a carboxylic acid anhydride moiety forming a pyrrolidine-2,5-dione backbone. Multiple reports have been published on the synthesis and applications of polyimide COFs that were highlighted in a recent review.⁹ Reaction conditions have employed solvothermal conditions¹⁰ and microwave irradiation (MW),¹¹ and the use of organic salt starting materials¹² or implementation of Lewis acids.¹³ These many recent reports have not adequately addressed how these various synthetic methods impact polymer molecular weight, morphology, defects and crystalline order. Since these COF materials are attractive for applications in membranes^{3,4,14,15} and liquid and gas separations,^{16,17} large COF flake sizes with high crystalline order are required.

In the synthesis of PI-COFs, there has been a focus on the use of amines with three-fold symmetry such as melamine (**MA**) and 1,3,5-tris(4-aminophenyl)benzene (**TAPB**), and their reactions with two-fold symmetric pyromellitic dianhydride (**PMDA**) and naphthalenetetracarboxylic dianhydride (**NTDA**) with two-fold symmetry (Figure 1). Multiple reports of the synthesis of these identical PI-COFs have often failed to even acknowledge/reference the previous syntheses to allow comparisons with previous

characterization data. To our knowledge, the first studies of **MA/PMDA** polymerization were by Hawthorne and Hodgkin in 1999 who reported issues with its polymerization;¹⁸ it was then reported by Tan in 2011,¹⁹ and again in 2012,²⁰ 2013²¹ and 2017.²² **MA/NTDA** was also reported by Tan in the same publication¹⁹ and also by others.²² COFs based on **TAPB** also have a rich history and were initially reported by Wang (2011),²³ again by others between 2014-2020,^{13,24,25} and yet again in 2021, which reported the “synthesis and characterization” of **TAPB/PMDA** and **TAPB/NTDA**.²⁶

Reports using a melamine precursor have significant disparities in the reported PI-COF characterization data that are purported to be identical. Therefore, we studied the formation of multiple PI-COFs, by variation of the reaction parameters that could lead to the nucleation and growth of the 2D framework. The parameters varied included the heating method, active stirring, temperature and organic salt precursor formation. The reactions were performed using traditional solvothermal conditions or microwave irradiation that have been known to produce different synthetic outcomes. In addition to the molecular precursors, organic salts of the two precursors were first synthesized and then reacted using both solvothermal and microwave heating to again evaluate the impact of heating method on polymer formation. All materials were characterized using FT-IR, PXRD, and TEM to determine functional groups, bulk crystallinity, and flake size and morphology, respectively with regard to the isolation method.²⁷ Our findings indicate considerable variance is observed in both the chemical composition and morphology of the product “COFs”. In addition, we report two additional “PI-COFs” that also show discrepancies from the expected reactions. It is the intent of this manuscript to illustrate that “PI-COFs” based on melamine monomers are likely producing **MA/PMDA** and **MA/NTDA** materials with significant errors in the 2D sheets. We first discuss the experimental evidence concerning these reactions in the results and discussion section. Next, we report mechanistic and modelling studies on small molecule model systems

^a Department of Chemistry, University of Wyoming, Laramie, WY 82071 USA

^b School of Energy Resources, University of Wyoming, Laramie, WY 82071 USA

* Corresponding Author: hoberg@uwyo.edu

Electronic Supplementary Information (ESI) available: See DOI: 10.1039/x0xx00000x

ARTICLE

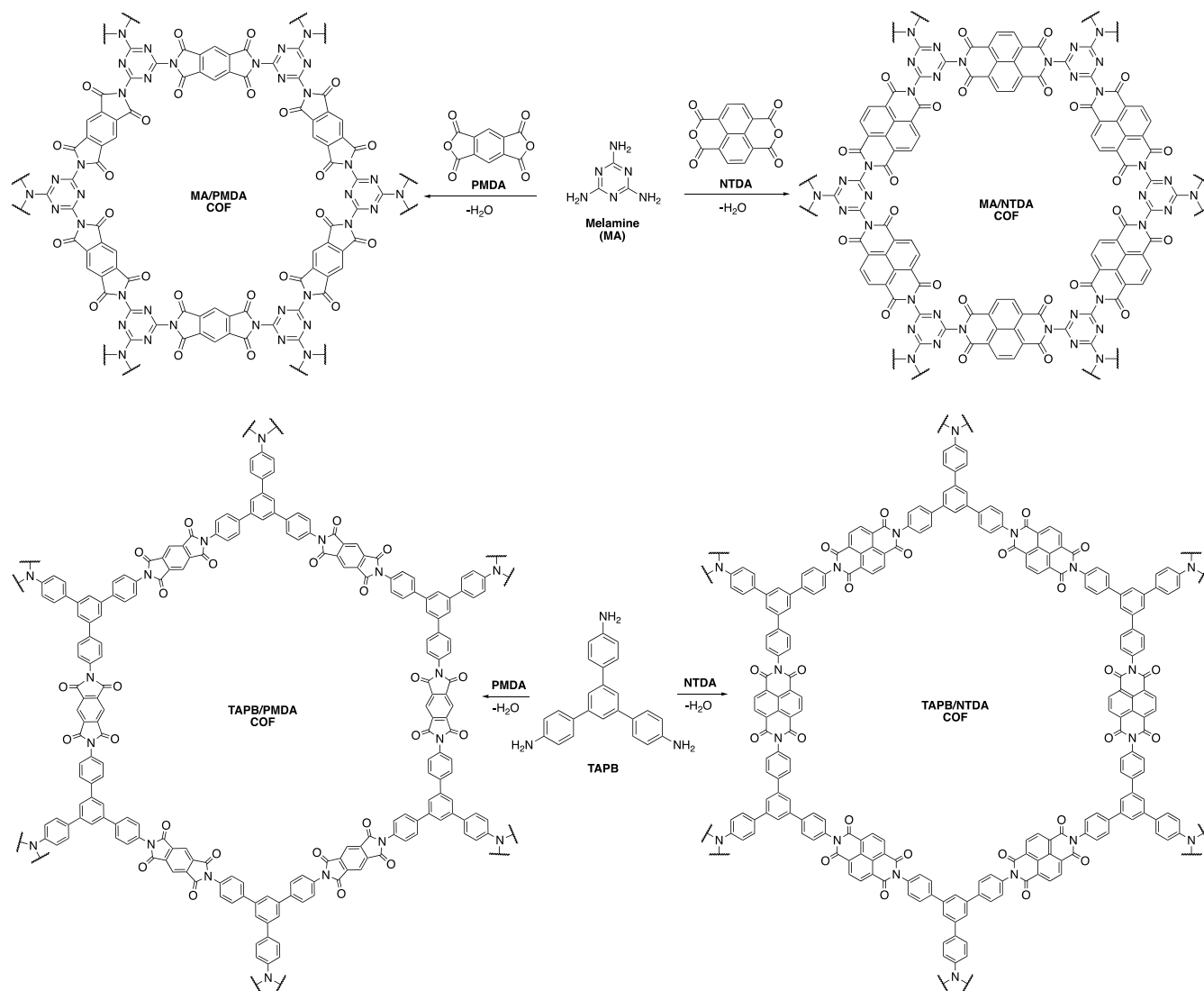
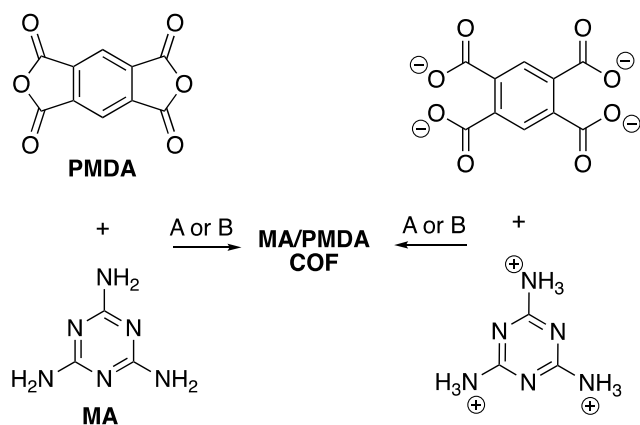


Figure 1. Example reactions for four COFs reported in the literature and studied in this paper.

along with titration experiments that lend insight into the errors that are occurring during the course of these reactions. Finally, to be clear, reactions involving the formation **TAPB/PMDA** and **TAPB/NTDA** COFs were reliably reproduced and do not appear to suffer from the poor nucleophilicity of the amine groups existing in the melamine monomer.

Results & Discussion: We started our study by reacting melamine (**MA**) and **PMDA** using the four different procedures as illustrated in Scheme 1 with and without stirring. Conditions A involved oven heating the monomers at 167 °C in a sealed tube with *N*-methyl pyrrolidone (NMP) as solvent for 3 days, while B employed microwave heating at 200 °C for two hours also in NMP.

Alternatively, the organic salts as starting materials were reacted under the same conditions. The starting organic salts were synthesized using methods adopted from literature preps and are detailed in the SI.¹² Optimization of the solvothermal temperature was achieved by testing temperatures of 167, 256, and 310 °C, where 167 °C was determined to be optimal based on PXRD and TEM results. Temperatures of 256 and 310 °C produced amorphous materials that were easily discernible (see SI figure S1).



Scheme 1. PI-COF MA/PMDA synthesis using neutral precursors (left) and salt precursors (right) with Conditions A: oven heating in a sealed ampule at 167 °C with NMP solvent for three days. Condition B: microwave heating at 200 °C with NMP solvent for two hours.

After Soxhlet and scCO_2 purification, TEM imaging of the PI-COF materials revealed significant morphological differences as shown in Figure 2. "COF" MA/PMDA, synthesized in the furnace, exhibited a thick 3D rhombohedral structure across multiple layers, indicated by the phase contrast image and produced no electron diffraction, which may be due to sample thickness (Figure 2A and 2B). These images probably indicate 3D salt crystallites. Whereas the MW reactions (Figure 2C and D) produced well defined thin flakes that did exhibit some electron diffraction (see supplemental). It appeared that the polymerization was not impacted by the ionic salt starting materials but rather the two conditions formed very different materials. Visually, the texture and color of the materials were also different as illustrated in the photographs (Figure 2G), that do not match the color reported in reference 18.²⁰

The FT-IR spectra of "COF" MA/PMDA were measured with the expectation that the carboxylic acid anhydride carbonyls and primary amine stretches in the starting material would disappear and the poly-imide COF carbonyls would appear. Figure 3 displays the FT-IR spectra for the oven reactions (A) and microwave reactions (B). The spectra of the salt starting materials are in the middle (blue) with the spectra of the products of each reaction above and below. The anhydride carbonyl stretch (1695 cm^{-1} for neutral and 1662 cm^{-1} for salt) moved to 1651 cm^{-1} for both furnace reactions using either neutral or salt starting materials, however the amine stretches were still apparent. In contrast, MW reactions displayed strong carbonyl stretches at 1727 and 1787 cm^{-1} as are expected for a proposed COF MA/PMDA phthalimide functionality. However, once again primary amine stretches ($3300\text{--}3500\text{ cm}^{-1}$) and amide NH stretches ($\sim 3100\text{ cm}^{-1}$) are observed in all cases.

To give further insights into the COF structures, given the contrasting TEM and FT-IR results, PXRD data was collected for each

COF and compared to starting material (Figure 3). Again, the diffractogram of the starting salt material is in the middle (blue) of each. The quite similar diffractograms for the furnace reactions using each type of starting materials in Figure 3C show the disappearance

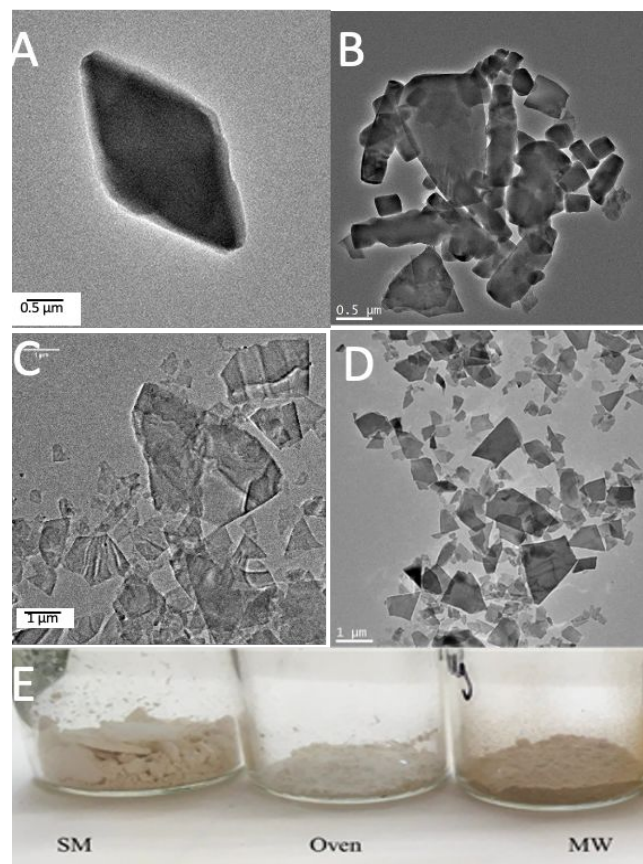


Figure 2. TEM images (A-D) and corresponding electron diffraction (E & F) of "COF" MA/PMDA with photographs of materials (G) from reaction of PMDA and melamine precursors as both neutral starting materials and salts. (A) furnace reaction of salt precursors, (B) furnace reaction of neutral precursors, (C) microwave reaction of salt precursors, (D) microwave reaction neutral precursors, Bottom photographs in (E) are of salt starting materials (left) and its reaction in both oven and microwave conditions.

of the small angle peak at 8.8 degrees (0.5 nm). In comparison, the MW reactions show the disappearance of the 11.7 degree (0.38 nm) peak from the starting material in each, but maintain the small angle peak at 8.8 degrees. The simulated PXRD for the MA/PMDA is also included in Figures 3 E and F for both an AA offset and AB pattern (AA stacking is illustrated in SI figure S2 along with calculations on varying interlayer distances). The simulated PXRD reveal some peaks that match the experimentally measured diffraction patterns, but none are in complete agreement, and peak intensity ratios are substantially different.

ARTICLE

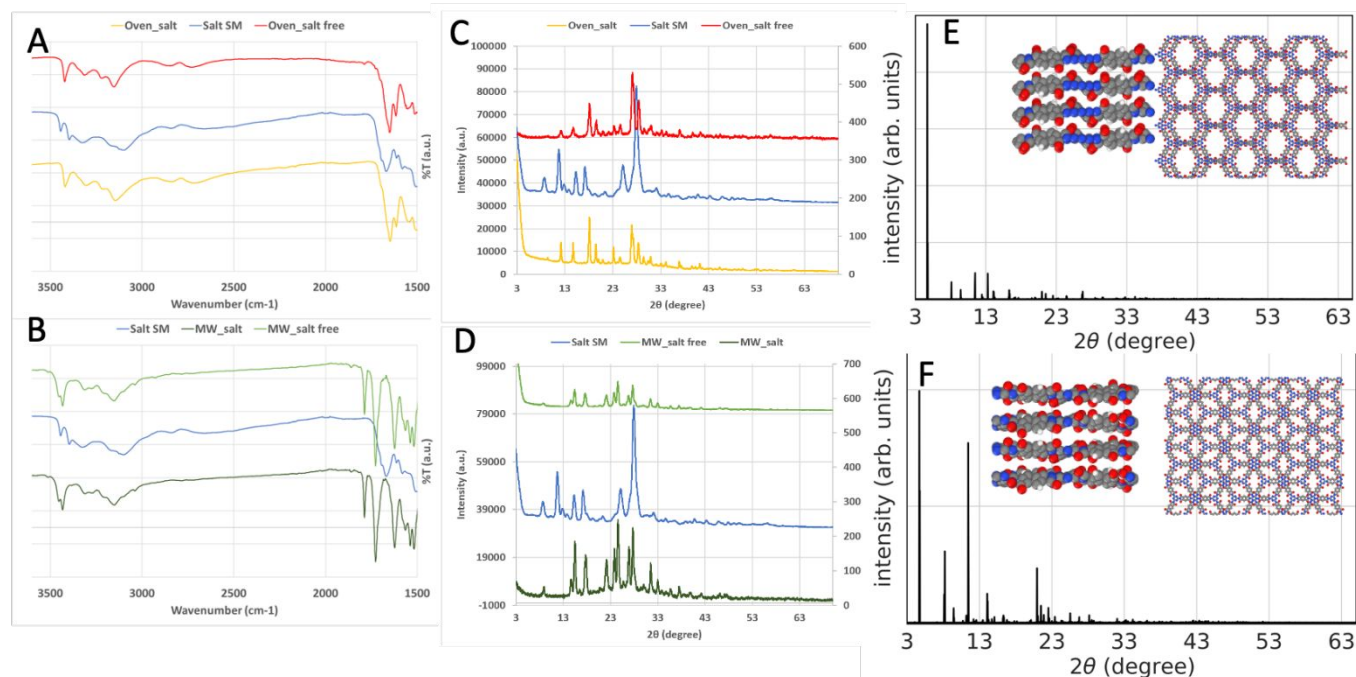


Figure 3. COF MA/PMDA comparisons between furnace and MW reactions using salt and neutral precursors. FT-IR data from synthesis via furnace (A) and MW reactions (B). PXRD data from synthesis via furnace (C) and MW reactions (D). Simulated PXRD assuming AA offset stacking (E), and AB stacking (F) (4.2 Å distance between layers). Side and top views of stacked COFs as insets.

Furthermore, comparison of the simulated PXRD to literature reported PXRDs (SI figure S3) do not show good agreement either. It should be noted that many sharp PXRD lines are the exception rather than the rule in most COF reports and in our case are indicative of salt formation where the coulombic packing forces are much stronger for producing ordered ionic materials.

Most notable are the differences between furnace and microwave reactions, and each characterization (TEM, IR and PXRD) confirms that different materials are being formed. TEM images and FT-IR spectra of the MW reactions indicate that this method might be optimal, however the PXRD illustrate that the MW method appeared to be producing an ordered but incomplete COF polymer. TEM images indicated COF flakes from oven reactions had greater thicknesses while the PXRD did indicate a new material was formed.

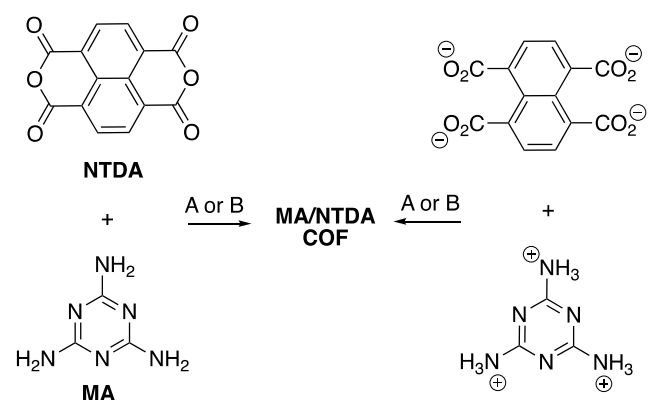
Finally, BET analysis was performed on samples from all four conditions (SI Figures S4-6). Products from both MW reactions had roughly the same N_2 adsorption and desorption behavior, however in the oven reaction the COFs formed from the neutral compounds had N_2 uptakes higher than that reported in reference 20, while that of the salt starting material showed no N_2 adsorption/desorption. All samples had ~ 40 g/cm³ or lower N_2 adsorption with greater than

expected pore size distributions of ~ 100 -200 Å. Thus, it is notable that in comparing our TEM, IR and PXRD data to that already published there is a lack of similarity with the published data as well as to each other.

Given the surprising differences in the above results, **NTDA** as the dianhydride was next investigated using the same conditions (Scheme 2). “COF” **MA/NTDA** was again characterized using TEM, FT-IR and PXRD, and again discrepancies in the characterization data from the different reaction conditions were observed.

TEM images of COF **MA/NTDA** (Figure 4) also exhibited significant differences related to the form of the starting material used in the reaction. Both MW and furnace reactions produced highly ordered COFs when using the neutral compounds (B and D), however reactions taking place with the use of organic salt precursor produced thick, plate-like flakes (A and C). Highly ordered material appeared in both images B and D with micron sized COF flakes showing hexagonal angles with electron diffraction spots that do not exhibit a hexagonal pattern (see supplemental). Thus, the formation of **MA/NTDA** appears to be impacted by the use of organic salt materials and relatively unaffected by the heating method. The

formation of dramatically different materials is illustrated by the photographs in Figure 4E.



Scheme 2. COF MA/NTDA synthesis using neutral precursors (left) and salt precursors (right) with Conditions A: oven heating in a sealed ampule at 167 °C with NMP solvent for 3 days. Condition B: microwave at 200 °C with NMP solvent for 2 hours.

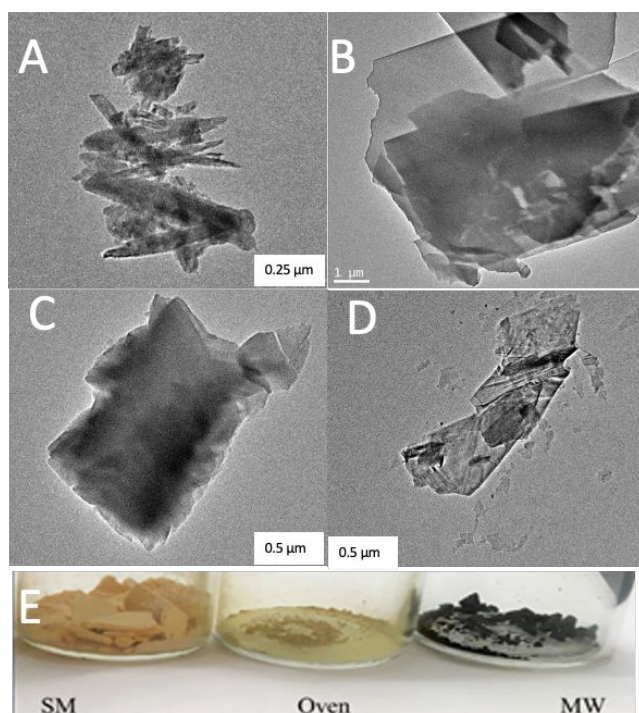


Figure 4. TEM images and corresponding electron diffraction of COF MA/NTDA. (A) furnace reaction of salt precursors, (B) furnace reaction of neutral precursors, (C) MW reaction of salt precursors, (D) MW reaction neutral precursors. (E) photographs using salt starting materials.

The obtained IR and PXRD spectra appeared to contain similar frequencies and diffraction peaks from all four reaction conditions (Figure 5). However, the oven PXRD spectrum of the neutral starting material gave strong indications that the salt precursors were actually being formed, while the reaction using salt precursors were not reacting. Only in the MW conditions did it appear that some conversion was taking place.

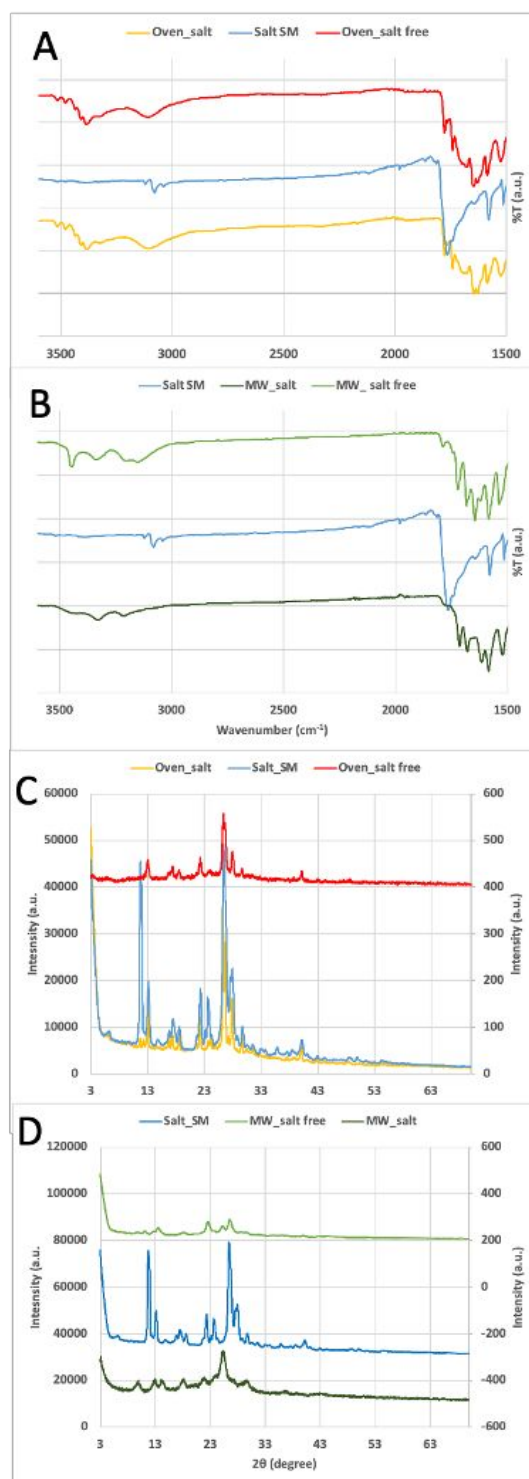


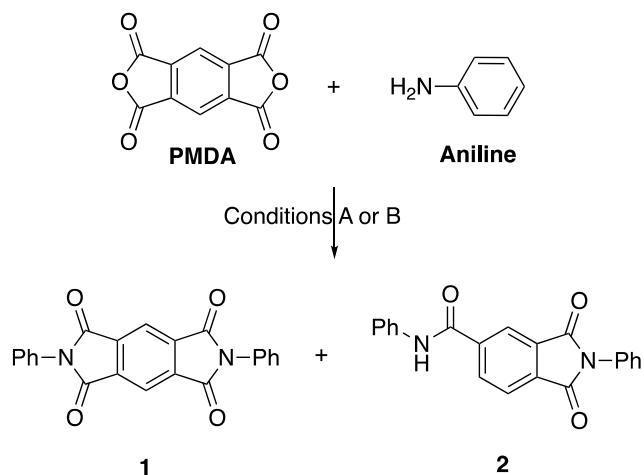
Figure 5. COF MA/NTDA FT-IR and PXRD comparisons between furnace reactions and microwave reactions. FT-IR data of COFs synthesized via furnace (A) and from MW reactions (B). PXRD data of COFs synthesized via furnace (C) and from MW reactions (D).

The results from the above studies led to the exploration of three additional polyimide-linked COFs using the same reactions and characterization methodology. These are outlined in the supplementary information and include reactions of pyrimidine triamine (PI) with PMDA (SI figure 7-9); and reaction of TAPB with

both **PMDA** (SI figure 10-12); and **NTDA** (SI figure 13-15). Noticeable differences were observed between thermal and MW conditions in the formation of the **PI/PMDA** COF as were observed for the above COFs in schemes 1 and 2. COFs formed by reacting **TAPB** with both **PMDA** or **NTDA** have been reported, as noted in the introduction, and we noticed very good agreement in these COFs with the data in the various publications and our reactions using isothermal conditions (comparisons to TEMs of starting salt materials can be made using SI figure S16-17). This is not surprising given the increased pore size resulting from the use of **TAPB**.

Model studies:

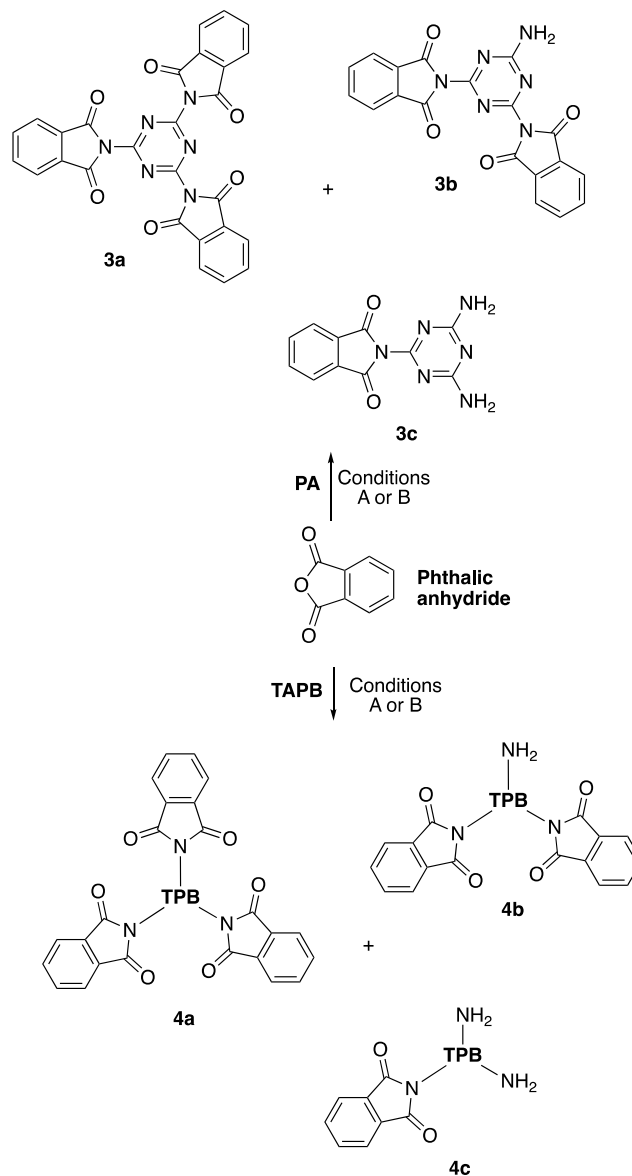
To understand and interpret the discrepancies in the formation of these PI-COFs, a series of model reactions were studied using small molecule counterparts due to the ease of using more definitive conventional characterization methods for small molecule products. Scheme 3 depicts the reaction of **PMDA** with aniline that is expected to produce **1** as the sole product. Using solvothermal conditions (oven at 167 °C for three days), a 79% yield of only diimide **1** was obtained. However, under microwave irradiation (200 °C for 2h) a 1:1 mixture of **1** and **2** was obtained in an overall 82% isolated yield. The decarboxylated imide **2** has been synthesized previously via alternate methods and this characterization data matched that of our isolated product **2** (SI, figures S18-21).²⁸ The formation of **2** was an unexpected result as a similar decarboxylation in COF forming reactions would greatly impact the formation of any highly ordered potential COFs studied here and in other reports using microwave conditions.²¹



Scheme 3. Model compound study using aniline as a surrogate for melamine and pyrimidine ($Ph = C_6H_5$).

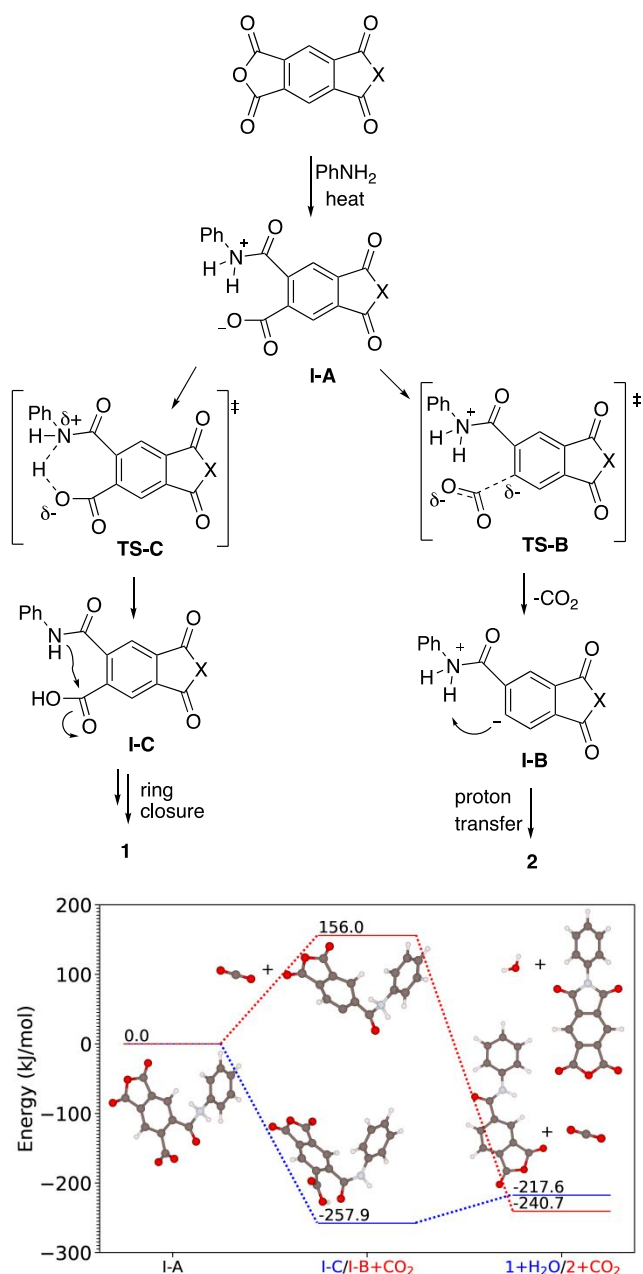
The reaction of the triamines with phthalic anhydride was also investigated to ascertain whether the required triimide formation was occurring. Both melamine and **TAPB** were reacted with three equivalents of phthalic anhydride solvothermally in an oven at 167 °C for three days and with microwave irradiation at 200 °C for both 2 hours and 6 hours (Scheme 4). The reaction components were analyzed using Matrix-Assisted Laser Desorption/Ionization (MALDI) mass spectrometry. In both the MW irradiation (2h and 6h reaction times) and the furnace reaction, a mixture of incomplete reaction

products was observed as illustrated with both **3a-3c** and **4a-4c** (SI figures S22-29). In the six-hour MW reaction, **3b** and **3c** were still observed. Surprisingly, the appearance of **4b** and **4c** were still observed even given the lack of repulsion that can occur in **4a**. Furthermore, decarboxylation products were observed from **4a** and **4b** using microwave heating, indicating this pathway is not an anomaly specific to **PMDA** and aniline as discussed for scheme 3.



Scheme 4. Model compound study using phthalic anhydride as a surrogate for **PMDA** and **NTDA** ($TPB = 1,3,5$ -triphenylbenzene).

A proposed mechanism is illustrated in Scheme 5, in which the initial attack of the amine leads to intermediate **I-A**. Decarboxylation leads to **I-B**, which picks up a proton to produce **2**. As no decarboxylation products were observed using solvothermal conditions, a computational study was performed on the energy differences of **I-A** leading to **I-B** or onto the imide **I-C** and **1**.

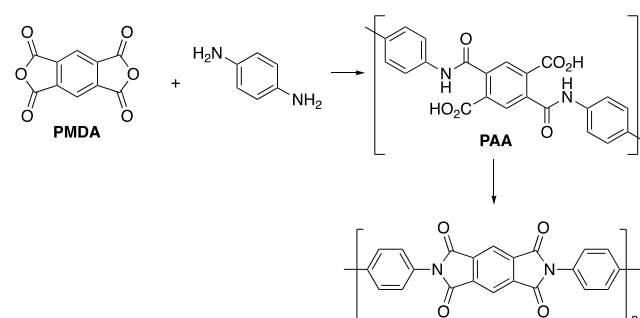


Scheme 5. Proposed mechanism for decarboxylation and conformational energies, X = Oxygen for the calculations but could be an imide during the course of the reaction.

The single-point calculations shown in scheme 5 were performed using the density functional theory (DFT) plane-wave code Quantum Espresso. We have used the Perdew-Zunger exchange-correlation functional within the local density approximation (LDA) and ultrasoft non-relativistic pseudopotentials for all DFT calculations. Calculation details are given in the methods section of the SI (figure S30). The energy profile depicted in scheme 5 indicates that the proposed intermediate state, I-B (+ CO₂), between I-A and 2 (+ CO₂), is far less energetically favorable (by an estimated 413.9 kJ/mol) than I-C. TS-C is the speculative transition state after I-A, leading to the amide C, and it should form spontaneously as an exothermic reaction from I-A given its lower energy (-257.9 kJ/mol). Based on Scheme 5, the

formation of 2 requires an overall higher energy than the formation of 1. Scheme 5 shows that different reaction kinetics take place in each route, as might reasonably be due to the variations in the approaches used to synthesize the materials. Most importantly, the calculations indicate that both products are stable, with the 2 + CO₂ products being more energetically favorable than 1 + H₂O. This is due to the slightly larger energy difference between the CO₂ and the H₂O molecules (56670.6 kJ/mol), compared to the final products, 1 and 2 (56647.5 kJ/mol). It should also be noted that the intermediate molecule I-C is thermodynamically stable. This illustrates that thermal heating is the preferred method as decarboxylation products were only observed using microwave conditions. The discrepancy and high energy difference indicate that localized energy absorptions are occurring in the MW that provide enough energy for the decarboxylation pathway.

Finally, acid-base titration studies of two different "COFs" were performed to establish and determine the amounts of carboxylic acid groups. In this study, an excess of triamine vs anhydride was used (vs the normal 1:1.5 ratio respectively) in attempts to line the edges of the flakes with amines. The titration consists of two steps (see SI figures S31 and 32) in which the COF is sonicated with NaOH to produce a sodium carboxylate and then back-titrated with HCl. The presence and quantity of carboxylate groups can be calculated by the consumption of the standardized HCl. The occurrence of carboxylic acid groups was unambiguously confirmed and using an approximate flake size of 1 micron an estimate of 1.5 COOH incorporation in each COF unit cell of the out of the 8 possible carboxylates was calculated. It should be noted that the edges of the 2D-COF sheets could contain unreacted carboxylic moieties. However, given the size of the sheets based on TEM and DLS, and the use of excess triamine, the presence of edge carboxylic acid moieties even if all ~1 micron flakes were terminated with carboxylic acid moieties would only account for a small fraction of the titrated carboxylates. Furthermore, many of the above IR spectra confirmed the presence of COOH moieties. The presence of carboxylic acid groups is also easily rationalized. Unterlass and co-workers reported the study on the polymerization of PMDA and phenylene diamine to produce straight-chain polyimide polymers, scheme 6.¹² Step-growth polymerization via the polyamic acid (PAA) is the known pathway for this pathway and is anticipated to be the pathway for MA/PMDA and MA/NTDA COF forming reactions. Thus, incomplete conversion to the polyimide establishes a third pathway for error propagation within these materials.



Scheme 6. Straight chain polymerization in polyimide formation.

To organize the data and methods for one of the PI-COFs, the characterization data and methods reported in the literature and herein for the purported formation of **MA/PMDA** are compiled in Table 1. This illustrates the inconclusive and inconsistent nature of the work related to this COF. Entries 1-4 illustrate the methods and type of starting materials employed while 5-13 tabulate the reported characterization data. Interestingly, the simulated PXRD is only reported herein (entry 6) and not a single experimental PXRD matches any of the three stacking modes that we simulated. Perhaps the closest evidence for formation of the proposed COF is found in reference 19, and yet several pieces of data indicate an imperfect COF. As stated above, **TAPB** based PI-COFs were confirmed to be the reported structures and can be reliably made. However, the use of single ring **MA** or **PI** triamines precursors allows for side reactions that prevent the formation of highly ordered crystalline materials. It can be postulated that the range of experimental data is likely due to the above issues (missing linkages, polyamic acid formation or decarboxylation in the MW conditions) to produce deviations from the desired materials. And as discussed elsewhere, errors within the COF material do influence the properties of the materials.^{29,30}

Table 1. Compilation of data for **MA/PMDA**

		Ref 19	Ref 20	Ref 21	Ref 22	This work
1	Thermal	✓	✓	-	✓	✓
2	MW	-	-	✓	-	✓
3	Salt S.M.	-	-	-	-	✓
4	Neutral SM	✓	✓	✓	✓	✓
5	PXRD exp					
6	PXRD sim	-	-	-	-	✓
7	TEM	-			-	
8	IR					
9	BET		-	-		
10	Titration	-	-	-	-	✓
11	Solids NMR		M	-	-	-
12	Elem. Anal.		M	-	-	-
13	TGA ^a	✓	✓	-	✓	✓

| = provided but inconclusive or inconsistent

M = provided and matches proposed structure

(-) = not provided or performed

✓ = performed

^a TGA:DSC data for COFs **MA/PMDA** and **MA/NTDA** indicated thermal stability up to 276 °C using solvothermal conditions, and 400 °C for MW (see SI figures S33-34).

Conclusions

We report a study of the synthesis of a series of polyimide-linked "COF"s by varying the reaction temperature, time, heating method and precursor type. The study illustrated significant variations in the proposed formation of the "COF"s. These variances can be explained by multiple factors that include: a) the nature of the triamine used, b) errors arising from decarboxylation side reactions, c) incomplete reactions at each of the amines in the triamine, d) formation of amide linkages with ortho carboxylic acid groups and e) formation of salts rather than COFs. In the case of a), triamines based on **MA** or **PA** must

adopt a three-dimensional shape leading to errors due to strain in the COFs. This strain would occur at the 120-degree imide linkage, where lone pairs from two carbonyls in conjunction with the electron rich melamine nitrogen are anticipated to exhibit charge-charge repulsion.¹⁰ With b), decarboxylation reactions appear to be related only to microwave reactions while furnace enabled reactions appear to be mostly free of this issue. The inherent advantage of oven reactions in this case is perhaps related to the higher locally available activation energy in microwave heating obtained to pass over the transition state barrier leading to decarboxylation. With respect to c), in reactions using **TAPB** a nearly error free COF formation occurs due to the ability for rotation in the triamine. However, even when using **TAPB** as the triamine in which free rotation can occur, and again perfect COF materials may likely not be produced if MW heating is used. While the use of ionic/salt starting materials prior to polymerization impacted the formation of a few COFs, the heating method appears to be far more important when applied to polymerization.

Finally, as noted, Hawthorne and Hodgkin reported studies of polyimide polymer formation with both **MA** and **PI** with **PMDA** in 1999.¹⁸ Using only ¹H NMR for polymer characterization, they deduced as we have that structural defects were "seriously impeding the formation of fully imidized derivatives". As stated in their conclusion "The results reported here clearly demonstrate that some heterocyclic polyamines may show non-ideal behavior in their condensation reactions with anhydrides, resulting in the incomplete conversion to imides, with a reduction in the molecular weights of oligomers containing them, and the formation of structural irregularities and abnormal groups. Whilst it is not suggested that the reactions of heterocyclic polyamines in other reported or claimed oligomer syntheses would exactly mirror those described here, the possible effects of low amine reactivity and the progressive deactivation during imidization are real, and cannot be ignored, as many previous workers would appear to have done." Thus, the "COFs" reported above using the triamines melamine and 2,4,6-triaminopyrimidine in the above mentioned references would be better viewed as amorphous polymers with high disorder, and future work should acknowledge the side-products and unreactive sites inherent in the resulting materials or methodology to avoid these pitfalls.

ASSOCIATED CONTENT

Supporting Information

All experimental and characterization data for the synthesis of the salt precursors and COFs, including characterization data.

Author Contributions

VAK performed all synthesis and characterization, MJW and LSO the computation studies, BAP and JOH supervised the project.

Conflicts of interest

“There are no conflicts to declare”.

Acknowledgements

Funding Sources

The authors acknowledge generous support from DOE-BES grant #DE-SC0020100 and a grant from the National Institute of General Medical Sciences (P20GM103432) from the National Institutes of Health. Calculations were performed with the Advanced Research Computing Center Teton Computing Environment (2018) at the University of Wyoming (<https://doi.org/10.15786/M2FY47>). LdSO further thanks Nitish Kumar for helpful discussions.

Notes and references

- P. Kuhn, M. Antonietti and A. Thomas, *Angew. Chem. Int. Ed.*, 2008, **47**, 3450–3453.
- H. Furukawa and O. M. Yaghi, *J. Am. Chem. Soc.*, 2009, **131**, 8875–8883.
- V. A. Kuehl, J. Yin, P. H. H. Duong, B. Mastorovich, B. Newell, K. D. Li-Oakey, B. A. Parkinson and J. O. Hoberg, *J Am Chem Soc*, 2018, **140**, 18200–18207.
- P. H. H. Duong, V. A. Kuehl, B. Mastorovich, J. O. Hoberg, B. A. Parkinson and K. D. Li-Oakey, *J Membr Sci*, 2019, **574**, 338–348.
- S.-Y. Ding, J. Gao, Q. Wang, Y. Zhang, W.-G. Song, C.-Y. Su and W. Wang, *J. Am. Chem. Soc.*, 2011, **133**, 19816–19822.
- T. Banerjee, F. Haase, G. Savasci, K. Gottschling, C. Ochsenfeld and B. V. Lotsch, *J. Am. Chem. Soc.*, 2017, **139**, 16228–16234.
- M. Dogru, M. Handloser, F. Auras, T. Kunz, D. Medina, A. Hartschuh, P. Knochel and T. Bein, *Angew. Chem. Int. Ed.*, 2013, **52**, 2920–2924.
- A. P. Cote, A. I. Benin, N. W. Ockwig, M. O’Keeffe, A. J. Matzger and O. M. Yaghi, 2005, **310**, 6.
- Y. Zhang, Z. Huang, B. Ruan, X. Zhang, T. Jiang, N. Ma and F. Tsai, *Macromol Rapid Commun*, 2020, 2000402.
- V. C. Wakchaure, A. R. Kottaichamy, A. D. Nidhankar, K. C. Ranjeesh, M. A. Nazrulla, M. O. Thotiyl and S. S. Babu, *ACS Appl Energy Mater*, 2020, **3**, 6352–6359.
- N. L. Campbell, R. Clowes, L. K. Ritchie and A. I. Cooper, *Chem Mater*, 2009, **21**, 204–206.
- M. J. Taublaender, M. Reiter and M. M. Unterlass, *Macromolecules*, 2019, **52**, 6318–6329.
- J. Maschita, T. Banerjee, G. Savasci, F. Haase, C. Ochsenfeld and B. V. Lotsch, *Angew Chem Int Ed*, 2020, **59**, 15750–15758.
- C. Zhang, B.-H. Wu, M.-Q. Ma, Z. Wang and Z.-K. Xu, *Chem Soc Rev*, 2019, **48**, 3811–3841.
- S. Yuan, X. Li, J. Zhu, G. Zhang, P. Van Puyvelde and B. Van der Bruggen, *Chem Soc Rev*, 2019, **48**, 2665–2681.
- V. Spaulding, K. Zosel, P. H. H. Duong, K. D. Li-Oakey, B. A. Parkinson, D. Gomez-Gualddron and J. O. Hoberg, *Mater Adv*, 2021, **2**, 3362–3369.
- R. W. Baker and B. T. Low, *Macromolecules*, 2014, **47**, 6999–7013.
- D. G. Hawthorne and J. H. Hodgkin, *High Perform Polym*, 1999, **11**, 315–329.
- Y. Luo, B. Li, L. Liang and B. Tan, *Chem Commun*, 2011, **47**, 7704.
- S. Chu, Y. Wang, Y. Guo, P. Zhou, H. Yu, L. Luo, F. Kong and Z. Zou, *J Mater Chem*, 2012, **22**, 15519.
- J.-D. Xiao, L.-G. Qiu, Y.-P. Yuan, X. Jiang, A.-J. Xie and Y.-H. Shen, *Inorg Chem Commun*, 2013, **29**, 128–130.
- T. Wang, R. Xue, H. Chen, P. Shi, X. Lei, Y. Wei, H. Guo and W. Yang, *New J Chem*, 2017, **41**, 14272–14278.
- Z. Wang, B. Zhang, H. Yu, G. Li and Y. Bao, *Soft Matter*, 2011, **7**, 5723.
- Q. Fang, Z. Zhuang, S. Gu, R. B. Kaspar, J. Zheng, J. Wang, S. Qiu and Y. Yan, *Nat Commun*, 2014, **5**, 1–8.
- L. Jiang, P. Wang, M. Li, P. Zhang, J. Li, J. Liu, Y. Ma, H. Ren and G. Zhu, *Chem Eur J*, 2019, **25**, 9045–9051.
- R. van der Jagt, A. Vasileiadis, H. Veldhuizen, P. Shao, X. Feng, S. Ganapathy, N. C. Habisreutinger, M. A. van der Veen, C. Wang, M. Wagemaker, S. van der Zwaag and A. Nagai, *Chem. Mater.*, 2021, **33**, 818–833.
- C. H. Feriante, S. Jhulki, A. M. Evans, R. R. Dasari, K. Slicker, W. R. Dichtel and S. R. Marder, *Adv. Mater.*, 2020, **32**, 1905776.
- K.-L. Wei, C.-H. Wu, W.-H. Huang, J.-J. Lin and S. A. Dai, *Macromolecules*, 2006, **39**, 12–14.
- F. Haase and B. V. Lotsch, *Chem Soc Rev*, 2020, **49**, 8469–8500.
- J. Brophy, K. Summerfield, J. Yin, J. Kephart, J. T. Stecher, J. Adams, T. Yanase, J. Brant, K. D. Li-Oakey, J. O. Hoberg and B. A. Parkinson, *Materials*, 2020, **14**, 71.